Single-shot transverse coherence measurements with Young's double pinholes at FLASH2

Journal of Physics Communications

OPEN ACCESS

RECEIVED
13 May 2020

REVISED
30 June 2020

ACCEPTED FOR PUBLICATION
7 July 2020

PUBLISHED
16 July 2020

PAPER

Single-shot transverse coherence measurements with Young's double pinholes at FLASH2

T Wodzinski[1], M Mehrjoo[2,3], M Ruiz-Lopez[2], B Keitel[2], M Kuhlmann[2], M Brachmanski[2], S Künzel[1], M Fajardo[1] and E Plönjes[2]

[1] GoLP/Instituto de Plasmas e Fusão Nuclear, Instituto Superior Técnico, 1049-001 Lisboa, Portugal
[2] Deutsches Elektronen-Synchrotron DESY, Notkestrasse 85, 22607 Hamburg, Germany
[3] Author to whom any correspondence should be addressed.

E-mail: masoud.mehrjoo@desy.de **and** thomas.wodzinski@tecnico.ulisboa.pt

Keywords: x-ray, Coherence, Free-Electron Lasers

Abstract

We measured the transverse coherence at FLASH2, a variable gap undulator line at the FLASH free-electron laser user facility at DESY in Hamburg. We demonstrate, theoretically and experimentally, a revised version of Young's double pinhole approach to perform single-shot, repeatable and non-invasive transverse coherence measurements. At beamline FL24 of FLASH2, the transverse coherence of pulses was systematically characterized at wavelengths of 8, 13.5 and 18 nm for different FEL source settings. We determine degrees of coherence of 57% to 87% in the vertical and horizontal direction, respectively. These measurements can facilitate the planning of novel, coherence-based experiments at the FLASH facility.

1. Introduction

Due to extraordinary properties of free-electron lasers (FELs) new opportunities transpire in many areas of natural science. Among the techniques that substantially profited from the advent of short wavelength coherent FEL radiation, we particularly address coherent diffractive imaging (CDI) [1–8], Fourier transform holography (FTH) [9–11], x-ray holographic microscopy (XHM) [12, 13], x-ray ptychography [14–17] and x-ray photon correlation spectroscopy (XPCS) [18–22]. The degree of transverse (spatial) coherence plays a crucial role in the success of these experiments. Thus, measuring the transverse coherence is essential to the operation of an FEL facility.

Over the last few years, there have been several attempts to characterize the coherence of self-amplified spontaneous emission (SASE) FEL sources in the soft and hard x-ray regimes [23–28]. Notably, in 2012, Singer *et al* [29] performed Young's double pinhole (YDP) experiment [30] at the FLASH1 undulator line.

In a YDP setup for FEL characterization, double pinholes were usually placed in the focus of the optics, which enabled planar illumination of each pinhole. Under this condition, the far-field interference pattern in an observation plane is only due to the optical path difference of light passing through pinholes. Thus, a straightforward analytical solution was given in [31] to extract the degree of transverse coherence from the measured interference pattern as a function of the pinhole separation. However, a typical focus on the micrometer scale made it impractical to perform a wide scan over the different pinhole separations. Additionally, the highly intense focused pulses destroyed the pinhole sets, requiring replacements after every single shot.

In this paper, we demonstrate an alternative approach, by illuminating a pinhole plate with a highly divergent beam downstream of the focus. This out-of-focus setup ensures a non-invasive, non-destructive illumination of the pinholes and allows a wide scan through the beam width, leading to precise transverse coherent measurements. However, the transition from planar to divergent illumination causes a significant change of the phase over each pinhole, which incorporates the beam's curvature into the interference pattern for a wide range of pinhole separations. The complexity of YDP experiments with a divergent illumination was

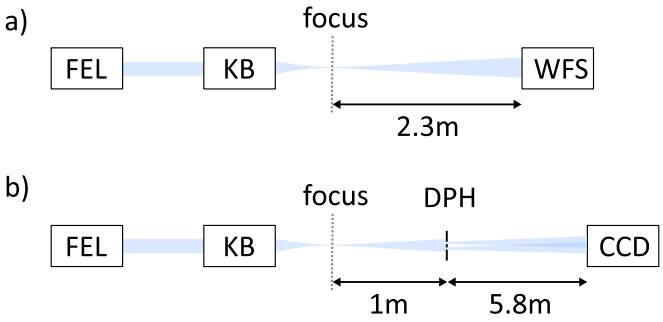

Figure 1. Experimental setup at beamline FL24 at FLASH2 for aligning the KB optics with a wave front sensor (WFS) (a) and for Young's double pinhole (DPH) measurements (b).

mentioned and partially investigated in [32]. In this work, we demonstrate two methods to determine the degree of transverse coherence of FELs with an out-of-focus YDP setup.

We performed a single-shot YDP experiment at the FLASH2 beamline [33], an additional variable-gap undulator line operational since 2016. The FLASH2 source generates radiation in the soft x-ray regime and operates as a SASE FEL which statistically behaves as a chaotic source. Due to the stochastic fluctuations, FLASH2 may not exhibit the same degree of transverse coherence as a fully coherent laser-like source, such as the seeded XUV FERMI FEL-2 source [34].

We present a general analytical solution to calculate the transverse coherence of out-of-focus FEL pulses and, additionally, we introduce the deconvolution method and its capabilities to extract the degree of transverse coherence. Utilizing both methods, we systematically characterized the degree of coherence for different FEL machine settings and different wavelengths of operation at FLASH2. Finally, we compare the analytical approach with the deconvolution method.

2. Experimental setup

Double pinholes (DPH) were illuminated near and downstream of a focus produced by Kirkpatrick-Baez (KB) focusing optics installed at beamline FL24 of FLASH2. Equipped with bendable mirrors, the focal length of the KB was set to 2 m while being inspected with a Hartmann wave front sensor (WFS) [35] (figure 1(a)). After the focus was established at the foreseen position, the end of the beamline was changed to replace the WFS with an XUV detector, positioned approximately 5.8 m from the position of the pinhole plate which was itself approximately 1 m downstream of the focus (figure 1(b)).

The pinhole plate consists of two sets of ten double pinhole pairs, oriented vertically and horizontally, respectively. The separation between the DPHs was ranging from 50 μm to 1557μm in several steps (see figure 2). The pinholes were manufactured using laser drilling with a diameter of approximately 10 μm.

The YDP plate was illuminated using various FEL source settings such as different number of active undulators, electron bunch charge and three different wavelengths of 8 nm, 13.5 nm and 18 nm. The FEL machine settings are listed in table 1.

Another plate with a phosphor coating and apertures for each pinhole pair was attached to the pinhole plate to allow a direct characterization of the FEL beam size with an optical camera by positioning the beam on a blank space between two pinhole pairs. The images were recorded using a Basler acA 1300–30 gm camera under 45° angle. The KB mirrors were adjusted such that the beam diameter was covering the maximum available pinhole separation. The second-moment width D4σ in horizontal and vertical direction was determined for each direct beam measurement based on ISO 11 146 method of variances [36]. Assuming a Gaussian intensity profile, the Full Width at Half Maximum (FWHM) is given as D $4\sigma \cdot 2.35/4$. For each FEL source setting the averaged beam widths are shown in figure 3 and also given later in table 2.

For each pinhole pair consecutive single-shot interference patterns were recorded using a Princeton Instruments PIXIS1024B XUV camera. Background images were collected by positioning the beam on the phosphor plate between two pinhole pairs. Single-shot information of pulse energies was provided by beam position monitoring [37, 38] installed in the beamline. Therefore, for each recorded single-shot a corresponding background image with the same energy could be determined. This allowed an accurate shot-to-shot analysis of the interference patterns.

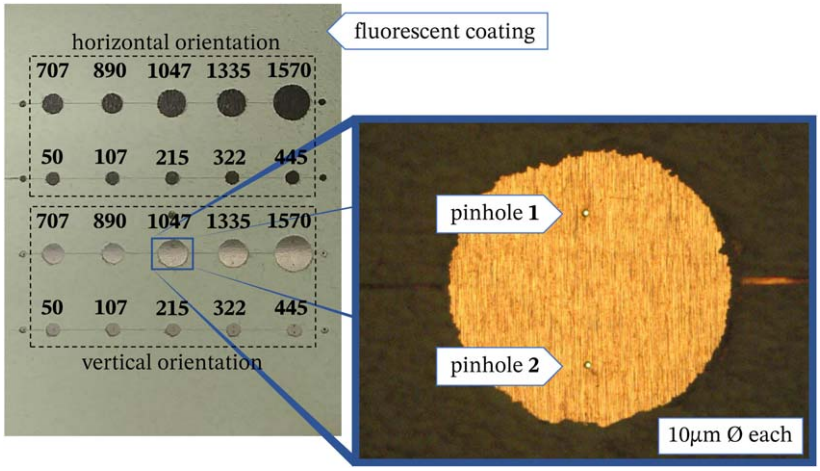

Figure 2. Double pinhole plate with an attached plate on top with a fluorescent phosphor coating. Ten pinhole pairs with increasing separation distances (indicated above each pair in μm) are shown in horizontal and vertical orientation. A microscope image shows an example of a pinhole pair. The pinholes have a diameter of 10 μm.

Table 1. FEL source settings of FLASH2 during the measurements. FLASH2 was running in single bunch mode, i.e. electron bunches, respectively photon pulses repeated at a rate of 10 Hz.

Machine setting	A	B	C	D
Undulators used	12	7	12	7
Tapering	none	none	last 6	none
Electron bunch charge/nC	0.15	0.20	0.20	0.15
Electron beam energy/MeV	1012.34	1042.20	1046.93	1010.59
Average pulse energy/μJ	45.1	68	111	66.7
Photon wavelength/nm	8	13.5	13.5	18

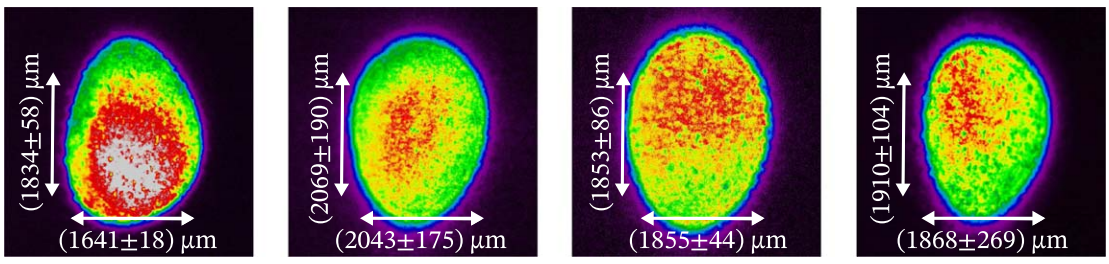

a) 8nm, 12 undulators b) 13.5nm, 12 undulators c) 13.5nm, 7 undulators d) 18nm, 7 undulators

Figure 3. Beam intensities on a plate with phosphor coating attached on top of the pinhole plate recorded with an optical beamline camera under a 45° angle. Figures (a) to (d) show example single shots for each FEL source setting. The D4σ width in horizontal and vertical direction is displayed for each setting.

3. Transverse coherence determination

3.1. Analytical fit

Figure 4 sketches the geometry of the YDP experiment at FLASH2. The focal plane of the KB optics is at $z_0 = 0$, and the pinhole pair is located downstream at position z_1. The electric field $E(\vec{s}, z_1)$, at the plane $\vec{s}\,(s_x, s_y)$, can be

Table 2. Determined coherence length $\xi_{(\mathrm{ver,hor})}$ and degree of coherence $\zeta_{(\mathrm{ver,hor})}$ through both methods as discussed in section 3. The values are given in horizontal and vertical direction, respectively. See table 1 for the FEL machine parameters.

Undulators	λ/nm	beam width $\sigma_{\mathrm{B,ver}}$ / μm	fitting ξ_{ver} / μm	deconvolution ξ_{ver} / μm	fitting ζ_{ver}	deconvolution ζ_{ver}
12	8	458.5 ± 14.5	748.0 ± 59.2	640.2 ± 80.9	0.63 ± 0.08	0.57 ± 0.09
12	13.5	517.3 ± 47.6	929.1 ± 121.0	1068.8 ± 116.7	0.67 ± 0.13	0.72 ± 0.11
7	13.5	463.3 ± 21.5	720.4 ± 19.9	825.5 ± 54.9	0.61 ± 0.06	0.67 ± 0.06
7	18	477.6 ± 26.1	1026.2 ± 62.3	1171.8 ± 37.7	0.73 ± 0.06	0.78 ± 0.04
Undulators	λ/nm	$\sigma_{\mathrm{B,\ hor}}$ / μm	ξ_{hor} / μm	ξ_{hor} / μm	ζ_{hor}	ζ_{hor}
12	8	410.3 ± 4.5	840.6 ± 42.7	828.5 ± 8.0	0.72 ± 0.08	0.71 ± 0.01
12	13.5	510.7 ± 43.7	779.3 ± 45.4	818.1 ± 23.8	0.61 ± 0.03	0.63 ± 0.02
7	13.5	463.8 ± 11.0	972.1 ± 30.3	1394.6 ± 75.0	0.72 ± 0.03	0.83 ± 0.08
7	18	467.0 ± 18.2	1395.7 ± 67.2	1642.9 ± 68.5	0.83 ± 0.05	0.87 ± 0.07

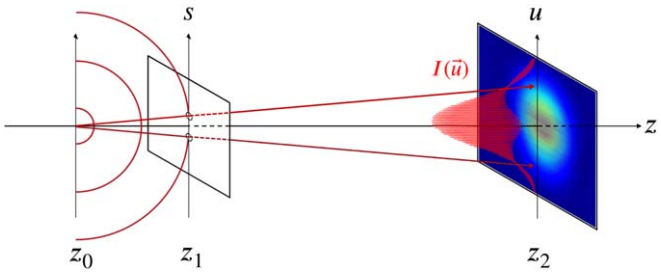

Figure 4. A YDP experiment with a divergent illuminating beam.

written as follows,

$$E(\vec{s},\, z_1) = E_0 \frac{k}{2\pi i} \frac{e^{ikz_1}}{z_1} \exp\left[ik\frac{|\vec{s}|^2}{2z_1}\right]. \tag{1}$$

We consider the free-space, paraxial propagation of the light through each pinhole to the measurement plane at z_2 to be determined by

$$E(\vec{u},\, z_2) = \left(\frac{k}{2\pi i}\right)^2 \frac{e^{ikz_2}}{\Delta z \cdot z_1} \exp\left[ik\frac{|\vec{u}|^2}{2\Delta z}\right] \int\int_{d/2-D/2}^{d/2+D/2} \exp\left[ik\frac{|\vec{s}|^2}{2z_M}\right] \exp\left[ik\frac{-2\,\vec{u}\cdot\vec{s}}{2\Delta z}\right] E_0 d\vec{s} \tag{2}$$

where d and D are the pinhole separation and diameter respectively, $\Delta z = z_2 - z_1$ is the relative distance between the two planes of propagation, and $z_M = \frac{z_1 \cdot \Delta z}{z_1 + \Delta z}$ identifies the effective propagation distance due to the divergent illumination of the pinholes.

We express the interference of the two fields at z_2 as

$$I(\vec{u}) = |E_1(\vec{u},\, z_2)|^2 + |E_2(\vec{u},\, z_2)|^2 + \gamma(E_1(\vec{u},\, z_2) \cdot E_2^*(\vec{u},\, z_2) + \text{c.c.}), \tag{3}$$

where γ is the degree of transverse coherence. We numerically simulated equation (3) as a fit function with z_1, D and d as the adjustable free parameters. We note that due to the pointing instability of the FLASH source a fixed z_1 did not lead to a convergence of the fits. For a stable source of radiation (such as seeded FELs) the variation in z_1 can probably be ignored. Additionally, an imbalanced illumination of pinholes was considered. Thus, equation (3) was fitted to all measured data by using the experimental values as the initialization of free parameters for the fits. A similar approach has been discussed in [39].

We call a heuristic measure that has a strong influence on the interference pattern interpretation, the dimensionless Fresnel number

$$F = \frac{((d + D)/2)^2}{\lambda \cdot z_M}. \tag{4}$$

With $F \ll 1$ we can omit the spherical phase term in equation (2) inside the integrand and apply the Fraunhofer diffraction formula [30, 31]. An analytical derivation of equation (3) under the Fraunhofer

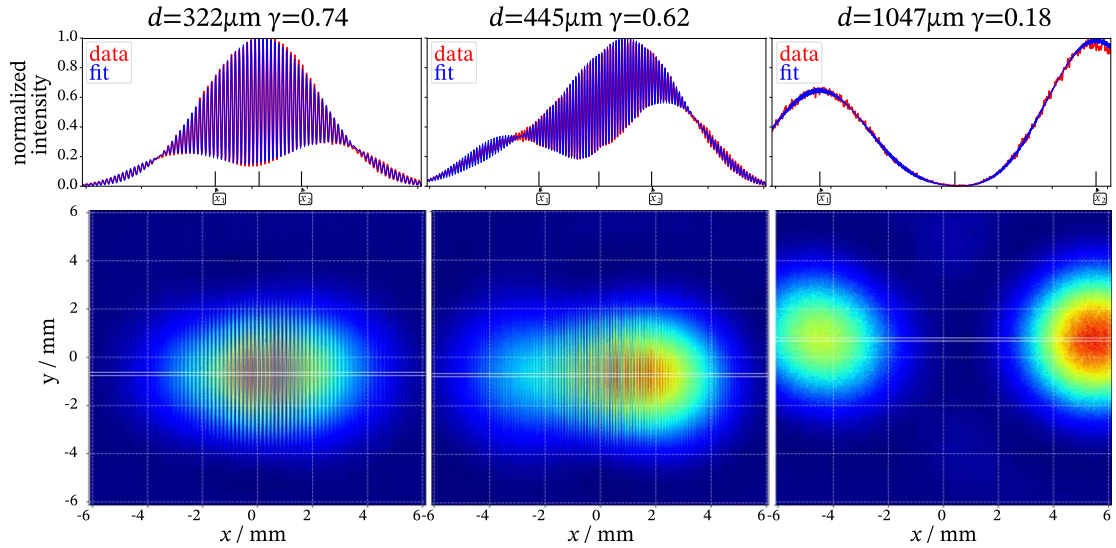

Figure 5. Examples of YDP experimental measurements with a divergent beam. The wavelength was 8 nm with 12 active undulators. Conventional fitting without considering the wave front curvature clearly failed to produce the same results.

approximation was given in [29] where the pinholes were illuminated with approximately planar waves at the focus of an x-ray focusing optics. In equation (4), for a given z_M and λ, $F \ll 1$ is satisfied for the small pinhole separations and equation (2) relies on the Fraunhofer approximation. On the other hand, for F values close to or larger than unity, the phase curvature of illumination is then sampled by the two pinholes and the assumption of a planar illumination is not held any longer. This can be understood by expanding the spherical phase factor as $\exp(x^2) = 1 + x^2 + \mathcal{O}(x^4)$. The first term of the expansion, within the integrand, results in the Fraunhofer formula and the second term involves the phase curvature over the pinhole width.

We chose a wide range of pinhole separations, spanning different values of F, to escalate the fit accuracy. Relying solely on the Fraunhofer approximation, we could only scan less than three pinhole separations over the out-of-focus beam whereas equation (3) enabled us to interpret data from a much wider range of pinhole separations.

In figure 5, we have shown three cases of interference pattern analysis where $F \geqslant 1$. The shown data were chosen to display the significant fluctuations of the FEL intensity. We discovered that for each separation the maximum of γ corresponds to the single shots illuminating both pinholes equally.

3.2. Deconvolution method

It has been shown by [40, 41] that a partially coherent intensity I_{pc} can be expressed as the convolution of a fully coherent intensity I_{fc} and the Fourier transformation of the transverse coherence function γ,

$$I_{\mathrm{pc}}(\vec{u}) = I_{\mathrm{fc}}(\vec{u}) * \mathscr{F}\{\gamma\}. \tag{5}$$

Therefore, we realized that the blind deconvolution approach (equation (5)) can be an alternative solution to resolve γ. We note that the blind deconvolution is a non-convex method and highly sensitive to the noise level. Thus, a proper background subtraction for each single shot is demanded. Here, in contrast to the previous section, we obtain the transverse coherence function explicitly without a need to fit.

For each measured intensity the transverse coherence extraction was performed with the algorithm shown in figure 6. The general steps in the algorithm are summarized as follows:

1. Initialize $\mathscr{F}\{\gamma(\vec{u})\}$ as a 2D-Gaussian:

$$\mathscr{F}\{\gamma\} = \hat{\gamma}^{k,i} = \exp\left[-\left(\frac{u_x^2}{2\sigma_x^2} + \frac{u_y^2}{2\sigma_y^2}\right)\right] \tag{6}$$

2. Deconvolve $I_{\mathrm{pc}}(\vec{u}) = I_{\mathrm{fc}}^{k,i}(\vec{u}) * \hat{\gamma}^{k,i}$

3. Compare the numerical convolution with the measured intensity using χ^2 -distance [42].

4. Update the horizontal and vertical root mean square (rms) width $\sigma_x^{k,i}$ and $\sigma_y^{k,i}$ of $\hat{\gamma}^{k,i}$.

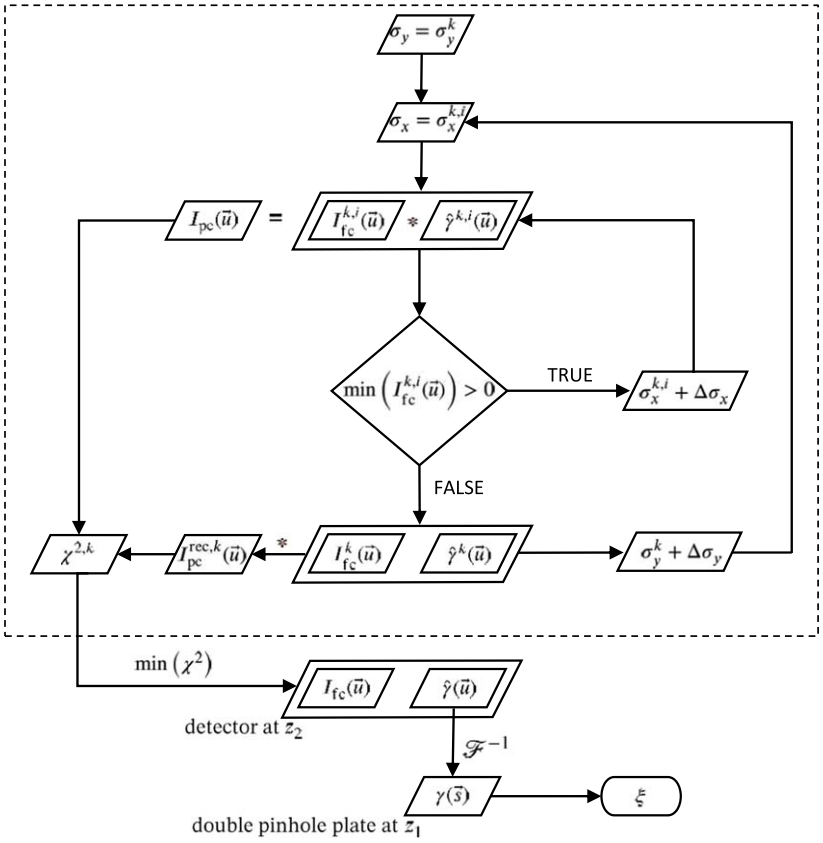

Figure 6. Deconvolution method to determine the coherence length ξ as the rms width of the degree of transverse coherence γ at the position of the pinhole plate z_1.

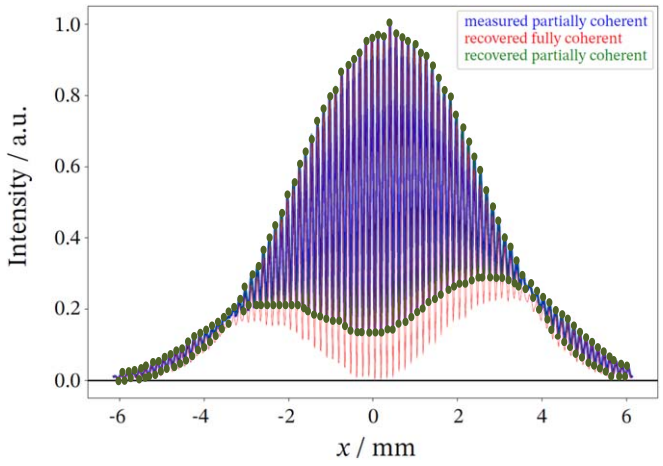

Figure 7. Measured intensity pattern (blue) of a double pinhole with a separation of $d = 322$ μm at a wavelength of $\lambda = 8$ nm. The retrieved fully coherent intensity is shown in red. The recovered partially coherent profile is in green. The determined coherence length is $\xi_x = 419.87$ μm in the horizontal and $\xi_y = 707.54$ μm in the vertical orientation.

5. Calculate $\mathscr{F}^{-1}\{\mathscr{F}\{\gamma\}\}$ to obtain the transverse coherence function.

We reconstruct the measured interference patterns by convolving both retrieved elements of the right hand side of equation (5). After scanning through various vertical and horizontal widths of $\mathscr{F}\{\gamma\}$ the optimal values were determined by the minimal χ^2 -distance. In figure 7 we have displayed the monitoring of the algorithm's accuracy. When the numerical convolution (green solid line) reaches the measured partially coherent intensity (blue solid line) the algorithm stops. The positivity constraint was applied to the coherent intensity (red solid line) to avoid non-physical solution.

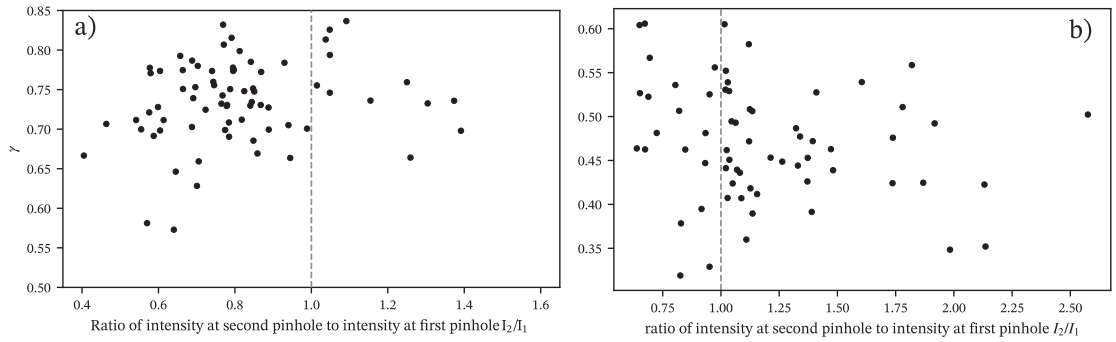

Figure 8. Determined values of the degree of transverse coherence γ versus different ratio of calculated intensities illuminating the pinholes. (a) and (b) correspond to the pinhole separations of 707 μm and 1335 μm at a wavelength of 13.5 nm.

We note that within the algorithm no symmetry constraint was imposed to equation (6). Due to different transverse electron bunch compressions at the FEL machine, an asymmetrical Gaussian distribution for γ was expected.

Also, within the measured datasets, we observed that the intensity distributions, though they transversely fluctuate, can be approximately described by a Gaussian distribution. Theoretically, Vartanyants *et al* [43] have shown that the Gaussian-Shell model would suffice to analyze the radiation at the FLASH facility. Therefore, we concluded, through the measured statistics, that the Gaussian-Shell model can adequately represent the radiation of the mentioned FEL source setting. Thus, for the deconvolution method, we define the degree of transverse coherence based on the aforementioned presumption of describing FLASH pulses in the Gaussian-Shell model. We notice that further studies with advanced methods such as ptychography [44] or modal-based diffraction imaging [45] would provide a more accurate representation of the FLASH2 pulses.

The size of a Gaussian beam can be characterized by the rms width [36] $\sigma_{B,\mathrm{hor}}$ in horizontal direction ($\sigma_{\mathrm{B,ver}}$ in vertical direction):

$$I(x) \propto \exp\left[-\frac{x^2}{2\sigma_{B,\mathrm{hor}}^2}\right] \tag{7}$$

With the knowledge of both, transverse coherence length and beam size, the degree of transverse coherence ζ_{hor} can be determined. In the framework of the Gaussian-Shell model [46] it is defined in horizontal and vertical direction, respectively, as

$$\zeta_{\mathrm{hor}} = \frac{\xi_{\mathrm{hor}}}{\sigma_{\mathrm{B,hor}}}\left(4 + \left(\frac{\xi_{\mathrm{hor}}}{\sigma_{\mathrm{B,hor}}}\right)^2\right)^{-1/2}. \tag{8}$$

4. Results and discussion

Broadly, both methods, namely analytical fits of the interference profiles and the deconvolution method, were used to determine the transverse coherence of the pulses with different FEL machine settings and pinhole separations. Due to the nature of the SASE process, an intrinsic shot-to-shot variation of intensity and position was observed. Thus, despite of a controlled alignment of the double-pinhole plate on the optical axis, unequal illumination of the pinholes was inevitable. The influence of unequal illumination on the determination of the transverse coherence has been studied in [47]. Addressing this, the highest value of γ for each pinhole separation through the measured dataset was taken. An illustration is shown in figure 8 for $d = 707$ μm and 1335 μm against the ratio of intensities at the two pinholes $\left(\frac{I_2}{I_1}\right)$. Observing more fluctuation for certain ratios can be attributed to an imperfect alignment of the pinholes from the optical axis (beam propagation axis). In fact, due to the rather small misalignment (figure 8(a)), to the left from the optical axis, more statistics have been measured for the ratio of $\left(\frac{I_2}{I_1} < 1\right)$. Also, for a different pinhole pair a misalignment to the right resulted in observing relatively more fluctuations in the right half of figure 8(b). The chaotic nature of SASE operating FELs and shot-to-shot fluctuations also have to be considered.

As discussed in [48], during the FEL amplification process the degree of transverse coherence improves until single-mode saturation is reached. A post-saturation condition (corresponding to the 12 undulators here) could result in growth of higher-order radiation modes, which degrades the transverse coherence. The degree of

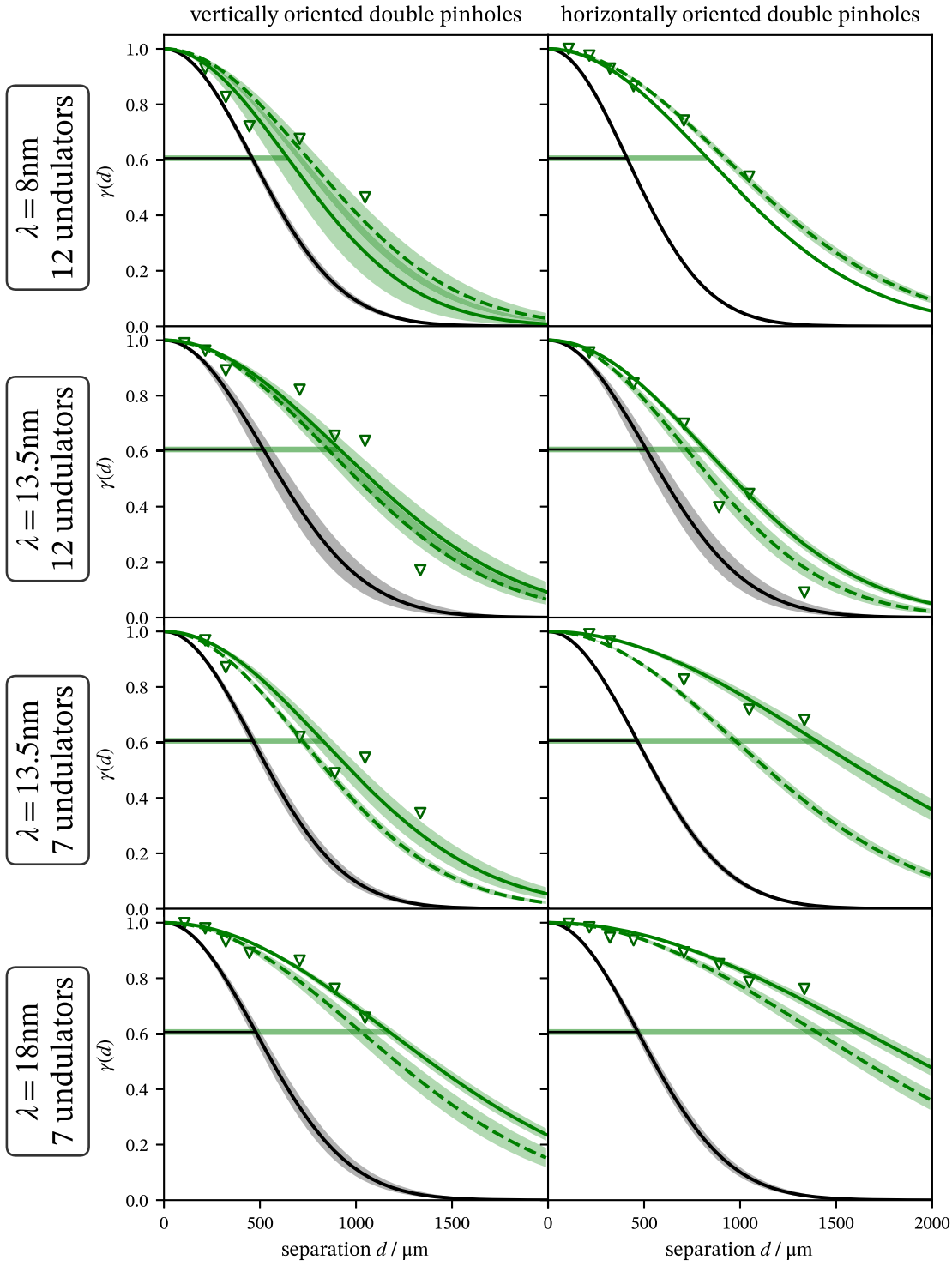

Figure 9. Degree of transverse coherence $\gamma(d)$ against pinhole separation d. Triangles are the determined γ values. The dashed line is from analytical modelling fit and the solid line represents the deconvolution method. The width of each colored area indicates the fit error. The green horizontal line represents the coherence length ξ. A Gaussian intensity profile is plotted in black with the rms width σ_B (plotted as black horizontal line) determined through D4σ method (see section 2 and table 2).

transverse coherence γ is plotted against the different pinhole separations d for all used FEL machine settings in figure 9.

It was found that for the pinhole separations larger than 1020 μm the analytical fitting model might not converge to a unique solution with reliable free-parameters of fitting. In that specific range, the deconvolution algorithm outperforms significantly the analytical fitting, and yields unique and reproducible solutions. Additionally, for pinhole separations less than 250 μm, we realized that the deconvolution method was trapped in a local minimum instead of reaching to the global minimum. Since in that length span the pulses have a very high degree of transverse coherence close to unity, deconvolving the measured profiles as stated in equation (5)

fails due to the negligible contribution of the transverse coherence function. In summary, for a wide scan of pinhole separations the two proposed methods complement, to precisely measure the transverse coherence of pulses.

The coherence length $\xi_{(\mathrm{ver,hor})}$ is calculated as the rms width of $\gamma(d)$. Using equation (8), we determine degrees of transverse coherence $\zeta_{(\mathrm{ver,hor})}$ in vertical and horizontal direction of 57% to 71% at a wavelength of 8 nm, 63 to 83% at 13.5 nm and 78% to 87% at 18 nm (see table 2). The given values are obtained through a wide scan covering pinhole separation widths from 107 μm to 1335 μm.

Practically, both methods yield comparable results to previously measured values at the FLASH1 facility. An exception was seen where the values for longer wavelengths are slightly smaller than expected.

5. Conclusion

We performed a single-shot YDP experiment to determine the transverse coherence of the FLASH2 facility, at the FL24 beamline. Due to the intense focus of the KB optics at FL24, the double-pinhole was installed far downstream of the focus, resulting in a divergent illumination of the pinhole pair. Incorporating a varying phase curvature over each pinhole, we introduced and demonstrated two reliable approaches to characterize the transverse coherence properties of an FEL source.

Our measurements, for three different wavelengths of 8 nm, 13.5 nm and 18 nm, involving an in-depth statistical analysis yielded a high degree of transverse coherence of approx. 60% to 90% with some variations for different wavelengths and FEL settings. The positional instability of the FEL pulses resulted in unequal irradiation of the pinholes. Its influence on the determined transverse coherence length was studied and accommodated into the data analysis. Our analysis shows that the FLASH2 source delivers highly coherent pulses as it was conceived for this facility. Further foreseen work on approaches such as mixed-state ptychography and speckle tracking will entail studying the partial coherence in detail. We believe that the presented approaches can be applied as a fast, on-line diagnostic tool at beamlines demanding the knowledge of transverse coherence.

Funding

Work funded by Portuguese FCT—Fundação para a Ciência e a Tecnologia, under grant PD/BD/105879/2014 (PD-F APPLAuSE) and IC&DT—AAC n. º 02/SAICT/2017—X-ELS 31 868. This work was supported by the European Union's Horizon 2020 Research and Innovation programme (VOXEL H2020-FETOPEN-2014-2015-RIA 665 207). This work has partially received funding from the European Union's Horizon 2020 Research and Innovation programme under Grant Agreement No 730 872.

ORCID iDs

T Wodzinski https://orcid.org/0000-0002-1081-7757
M Mehrjoo https://orcid.org/0000-0001-8003-286X

References

[1] Chapman H N *et al* 2006 *Nat. Phys.* **2** 839–43
[2] Williams G J, Quiney H M, Peele A G and Nugent K A 2007 *Phys. Rev.* B **75** 104102
[3] Abbey B, Nugent K A, Williams G J, Clark J N, Peele A G, Pfeifer M A, de Jonge M and McNulty I 2008 *Nat. Phys.* **4** 394–8
[4] Gutt C *et al* 2009 *Phys. Rev.* B **79** 212406
[5] Seibert M M *et al* 2011 *Nature* **470** 78–81
[6] Zürch M, Jung R, Späth C, Tümmler J, Guggenmos A, Attwood D, Kleineberg U, Stiel H and Spielmann C 2017 *Sci. Rep.* **7** 5314
[7] Huang C F *et al* 2018 *Nanoscale* **10** 2820–4
[8] Giewekemeyer K *et al* 2019 *IUCrJ* **6** 357–65
[9] Eisebitt S, Lüning J, Schlotter W F, Lörgen M, Hellwig O, Eberhardt W and Stöhr J 2004 *Nature* **432** 885–8
[10] Streit-Nierobisch S *et al* 2009 *J. Appl. Phys.* **106** 083909
[11] Schaffert S, Pfau B, Geilhufe J, Günther C M, Schneider M, von Korff Schmising C and Eisebitt S 2013 *New J. Phys.* **15** 093042
[12] Stickler D *et al* 2010 *Appl. Phys. Lett.* **96** 042501
[13] Lider V V 2015 *Phys. Usp.* **58** 365–83
[14] Rodenburg J M, Hurst A C, Cullis A G, Dobson B R, Pfeiffer F, Bunk O, David C, Jefimovs K and Johnson I 2007 *Phys. Rev. Lett.* **98** 034801
[15] Bunk O, Dierolf M, Kynde S, Johnson I, Marti O and Pfeiffer F 2008 *Ultramicroscopy* **108** 481–7
[16] Rose M *et al* 2015 *J. Synchrotron Radiat.* **22** 819–27
[17] Pfeiffer F 2017 *Nat. Photonics* **12** 9–17
[18] Grübel G, Stephenson G B, Gutt C, Sinn H and Tschentscher T 2007 *Nucl. Instrum. Methods Phys. Res., Sect. B* **262** 357–67

[19] Gutt C, Stadler L M, Duri A, Autenrieth T, Leupold O, Chushkin Y and Grübel G 2008 *Opt. Express* **17** 55
[20] Hruszkewycz S O *et al* 2012 *Phys. Rev. Lett.* **109** 185502
[21] Roseker W *et al* 2018 *Nat. Commun.* **9** 1704
[22] Zhang Q, Dufresne E M and Sandy A R 2018 *Curr. Opin. Solid State Mater. Sci.* **22** 202–12
[23] Ischebeck R *et al* 2003 *Nuclear Instruments and Methods in Physics Research section A: Accelerators, Spectrometers,,Detectors and Associated Equipment* **507** (1-2) 175–80
[24] Vartanyants I A, Mancuso A P, Singer A, Yefanov O M and Gulden J 2010 *J. Phys. B: At. Mol. Opt. Phys.* **43** 194016
[25] Mai D D *et al* 2013 *Opt. Express* **21** 13005
[26] Inoue I, Tono K, Joti Y, Kameshima T, Ogawa K, Shinohara Y, Amemiya Y and Yabashi M 2015 *IUCrJ* **2** 620–6
[27] Yun K *et al* 2019 *Sci. Rep.* **9** 3300
[28] Cho D, Yang J, Soo Kim S, Nam D, Park J, Kim S, Tono K, Yabashi M, Ishikawa T and Song C 2019 *Opt. Express* **27** 19573
[29] Singer A *et al* 2012 *Opt. Express* **20** 17480–95
[30] Goodman 2015 *Statistical Optics* 2nd edn (New York: Wiley)
[31] Born M, Wolf E and Bhatia A B 2002 *Principles of Optics* (Cambridge: Cambridge University Press)
[32] Bartels R A, Paul A, Green H, Kapteyn H C, Murnane M M, Backus S, Christov I P, Liu Y, Attwood D and Jacobsen C 2002 *Science* **297** 376–8
[33] Plönjes E, Faatz B, Kuhlmann M and Treusch R 2016 *AIP Conf. Proc.* **1741** 020008
[34] Gorobtsov O Y *et al* 2018 *Nat. Commun.* **9** 4498
[35] Keitel B, Plönjes E, Kreis S, Kuhlmann M, Tiedtke K, Mey T, Schäfer B and Mann K 2016 *J. Synchrotron Radiat.* **23** 43–9
[36] ISO 2005-01 ISO 11 146: Lasers and Laser-Related Equipment—Test Methods for Laser Beam Widths, Divergence Angles and Beam Propagation Ratios https://www.iso.org/obp/ui/#iso:std:iso:11146:-1:ed-1:v1:en
[37] Tiedtke K *et al* 2008 *J. Appl. Phys.* **103** 094511
[38] Tiedtke K *et al* 2013 Challenges for detection of highly intense FEL radiation: Photon beam diagnostics at FLASH1 and FLASH2 *Proc. XXXV Free-Electron Laser Conf* pp 417–20978-3-95450-126-7
[39] Saleh B and Teich M 2007 *Fundamentals of Photonics* (*Wiley Series in Pure and Applied Optics*) (New York: Wiley)
[40] Vartanyants I A and Robinson I K 2001 *J. Phys. Condens. Matter* **13** 10593
[41] Clark J N, Huang X, Harder R and Robinson I K 2012 *Nat. Commun.* **3** 993
[42] Brunelli R and Mich O 2001 *Pattern Recognit.* **34** 1625–37
[43] Vartanyants I A and Singer A 2010 *New J. Phys.* **12** 035004
[44] Schropp A *et al* 2013 *Sci. Rep.* **3** 1633
[45] Karbeyaz E and Rappaport C M 2009 *J. Opt. Soc. Am.* A **26** 19–29
[46] Mandel L and Wolf E 1995 *Optical Coherence and Quantum Optics* (Cambridge: Cambridge University Press)
[47] Vartanyants I A *et al* 2011 *Phys. Rev. Lett.* **107** 144801
[48] Schneidmiller E and Yurkov M 2016 Transverse Coherence and Fundamental Limitation on the Pointing Stability of X-ray FELs *VII International Particle Accelerator Conf. (IPAC'16) (Busan, Korea, May 8-13, 2016)* pp 735–7